

Progressive Image Super-Resolution via Neural Differential Equation

Seobin Park and Tae Hyun Kim

Hanyang University, Seoul, South Korea

{seobinpark, taehyunkim}@hanyang.ac.kr

Abstract

We propose a new approach for the image super-resolution (SR) task that progressively restores a high-resolution (HR) image from an input low-resolution (LR) image on the basis of a neural ordinary differential equation. In particular, we newly formulate the SR problem as an initial value problem, where the initial value is the input LR image. Unlike conventional progressive SR methods that perform gradual updates using straightforward iterative mechanisms, our SR process is formulated in a concrete manner based on explicit modeling with a much clearer understanding. Our method can be easily implemented using conventional neural networks for image restoration. Moreover, the proposed method can super-resolve an image with arbitrary scale factors on continuous domain, and achieves superior SR performance over state-of-the-art SR methods.

1 Introduction

Image super-resolution (SR) is a classic low-level vision task that aims to recover a high-resolution (HR) image from a given low-resolution (LR) input image. For several decades, a large volume of literature documents the high demand of SR technique in various vision applications. However, SR problem still remains a challenge and is difficult to solve because it is a highly ill-posed inverse problem.

With the recent development of deep learning technology, numerous deep-learning-based SR methods [Dong *et al.*, 2015; Kim *et al.*, 2016b; Zhang *et al.*, 2018] have been presented, and they have shown plausible results. Specifically, SRCNN [Dong *et al.*, 2015] is the first SR approach using convolutional neural networks (CNNs), and it shows that a three-layered CNN can outperform traditional SR approaches by learning a complex function that maps LR images to HR ones. Since then, a large number of follow-up studies with neural networks have been put forward, and they have elevated the SR performance significantly by exploiting much deeper and more complicated neural architectures to model the complex mapping from the LR to HR images [Kim *et al.*, 2016b; Zhang *et al.*, 2018; Li *et al.*, 2019; Hu *et al.*, 2019].

To further improve the SR performance, many researchers have attempted to restore the high-quality image by recovering the fine details of the LR input image progressively [Haris *et al.*, 2018; Li *et al.*, 2019]. Many previous works hinged on this progressive SR procedure are based on a variant of feedback network in the human visual system [Zamir *et al.*, 2017], and they show satisfactory SR results. However, owing to lack of theoretical clarity on the progressive system, these approaches need to develop a well-engineered method. For example, the number of iterations for the gradual refinements [Tai *et al.*, 2017] and complicated learning strategies [Li *et al.*, 2019] as well as the network architectures [Haris *et al.*, 2018] are considered to improve the SR performance.

Several researchers have conducted studies on differential equations to solve the image restoration problems [Chen and Pock, 2016; Chen *et al.*, 2005]. They also have developed progressive approaches, but these approaches are limited to modeling the prior and/or likelihood models.

In this study, we introduce an ordinary differential equation (ODE) that describes an explicitly defined progressive SR procedure from the LR to HR images via a neural network. In particular, we reconstruct the HR image by numerically solving the initial value problem originated from the proposed ODE formulation, given the LR image as an initial condition. With the aid of the proposed ODE, our method eases implementation using conventional restoration networks and ODE solvers without any exertion to improve the performance. Furthermore, by simply changing the initial condition of our formulation at the test-time, ours can naturally handle a continuous-valued scale factor. Extensive experiments demonstrate the superiority of the proposed method over state-of-the-art SR approaches. In summary, our main contributions are as follows:

- We introduce a new ODE-based formulation that allows the SR task to be performed progressively.
- Unlike conventional progressive SR methods, we need not additional efforts in modeling and training with the clarity of our formulation.
- Our method can handle arbitrary scale factors and achieve superior performance over state-of-the-art SR methods.

2 Related Works

2.1 Single Image Super-Resolution

Recent works on single image super-resolution (SISR) focus on learning mapping functions between LR and HR image patches. SRCNN [Dong *et al.*, 2015] proposed to learn the non-linear mapping from LR image to HR image using a CNN model for the first time. VDSR [Kim *et al.*, 2016b] increased the depth of CNN to model more complex LR-HR mappings. Recent studies have applied different kinds of skip connections to ease the optimization process [Lim *et al.*, 2017; Zhang *et al.*, 2018].

Parallel to devising improved feed-forward CNN architectures, many attempts have been done to develop SISR methods that can be better applied to real-world situations. RealsLR [Cai *et al.*, 2019] proposed a more realistic degradation model to make more natural training dataset and presented a new method to cope with the given degradation settings. Meta-SR [Hu *et al.*, 2019] proposed Meta-Upscale module to handle arbitrary scale factors for SISR.

2.2 Progressive Image Restoration

Progressive approaches have been proven to perform well in low-level vision tasks. In addition to learning a complex non-linear mapping of a low-quality image to a high-quality one, these approaches decompose this process into multiple steps and iteratively refine the output images [Kim *et al.*, 2016a; Tai *et al.*, 2017; Haris *et al.*, 2018; Li *et al.*, 2019]. DBPN [Haris *et al.*, 2018] proposed a dedicated neural network design that provides an iterative error correcting mechanism to address mutual dependencies of LR and HR images. SRFBN [Li *et al.*, 2019] proposed an efficient recurrent neural network that employs the feedback mechanism, which iteratively improves the input of the network in each step. However, these methods do not have a clear underlying formulation or theoretical analysis on the progressive image restoration process, which consequently require a large amount of engineering to develop the neural architectures [Li *et al.*, 2019; Haris *et al.*, 2018] and specialized training strategies [Li *et al.*, 2019; Kim *et al.*, 2016a]. LapSRN [Lai *et al.*, 2017] can produce large SR results (e.g., x8) with intermediate SR results (e.g., x2, x4), but it can only handle the pre-determined discrete scale factors such as x2, x4, and x8.

2.3 Neural Ordinary Differential Equation

Recently, many attempts have been done to integrate differential formulations and deep learning methodologies. These attempts have led to neural ordinary differential equations (NODE) [Chen *et al.*, 2018]. NODE is a new family of deep neural network models that parameterizes a differential form using a neural network and produces the output by using an ODE solver. Meanwhile, differential equations have often been involved in image restoration task by modeling non-linear reaction-diffusion and total variation schemes [Chen and Pock, 2016; Rudin *et al.*, 1992]. Such is also the case in deep-learning-based image restoration methods. [He *et al.*, 2019] designed new neural network architectures inspired by the differential equation solving process, such as Leapfrog and Runge–Kutta approaches. In particular, to solve the SR

problem, [Scao, 2020] utilized NODE as a part of neural architecture with an integration. However, the interval of the integral is not fixed (open) and they did not present any concrete formulation on the intermediate images involved in the progressive SR process. Consequently, they need to empirically speculate the optimal neural architecture and the integration interval.

3 Proposed Method

In this section, we present a new neural approach for the progressive SR reconstruction. We first formulate the SR problem as a progressive SR process with an ODE. We then elaborate how to perform SR with the proposed formulation and how to train it.

3.1 Progressive Super-Resolution Formulation

Existing SR methods utilizing progressive SR process [Lai *et al.*, 2017; Haris *et al.*, 2018; Li *et al.*, 2019] are based on iterative multi-stage approaches and can be viewed as variants of the following:

$$I_n = g_{n-1}(I_{n-1}) \quad (n \leq N), \quad (1)$$

where n denotes the iteration step, I_0 denotes the given initial input LR image, and I_n is the iteratively refined image from its previous state I_{n-1} . These approaches typically produce multiple intermediate HR images during the refinement, and the rendered image at the last N -th iteration [Tai *et al.*, 2017; Li *et al.*, 2019] or a combined version of the multiple intermediate images ($\{I_n\}_{1 \leq n \leq N}$) [Kim *et al.*, 2016a; Haris *et al.*, 2018] becomes the final SR result. Although these previous progressive methods show promising SR results, they still have some limitations. First, these methods need plenty of time and effort in determining the network configurations including the number of progressive updates N and hyper-parameter settings, and designing cost functions to train the SR networks g . In addition, well-engineered and dedicated learning strategy, such as curriculum learning [Li *et al.*, 2019] and recursive supervision [Kim *et al.*, 2016a], is required for each method. This complication comes from the lack of clear understanding on their intermediate image states $\{I_n\}$. To alleviate these problems, we formulate the progressive SR process with a differential equation. This allows us to implement and train the SR networks in an established way while outperforming the performance of conventional progressive SR process.

Assume that $(I_{HR}) \downarrow_t$ is a downsampled version of a ground-truth clean image I_{HR} using a traditional SR kernel (e.g., bicubic) with a scaling factor $\frac{1}{t}$. We then define $\mathcal{I}(t)$ by upscaling $(I_{HR}) \downarrow_t$ using that SR kernel with a scaling factor t so that I_{HR} and $\mathcal{I}(t)$ have the same spatial resolution (see the illustration of “Generating LR image” in Figure 1(a)). Note that $t \geq 1$, and $\mathcal{I}(1)$ denotes the ground-truth clean image I_{HR} . To model a progressive SR process, we first estimate the high-frequency image residual with a neural network. Specifically, when t is a conventional discrete-scaling factor (e.g., x2, x3, and x4), image residual between $\mathcal{I}(t)$ and $\mathcal{I}(t-1)$ can be modeled using a neural network f_{discrete} as:

$$\mathcal{I}(t-1) - \mathcal{I}(t) = f_{\text{discrete}}(\mathcal{I}(t), t). \quad (2)$$

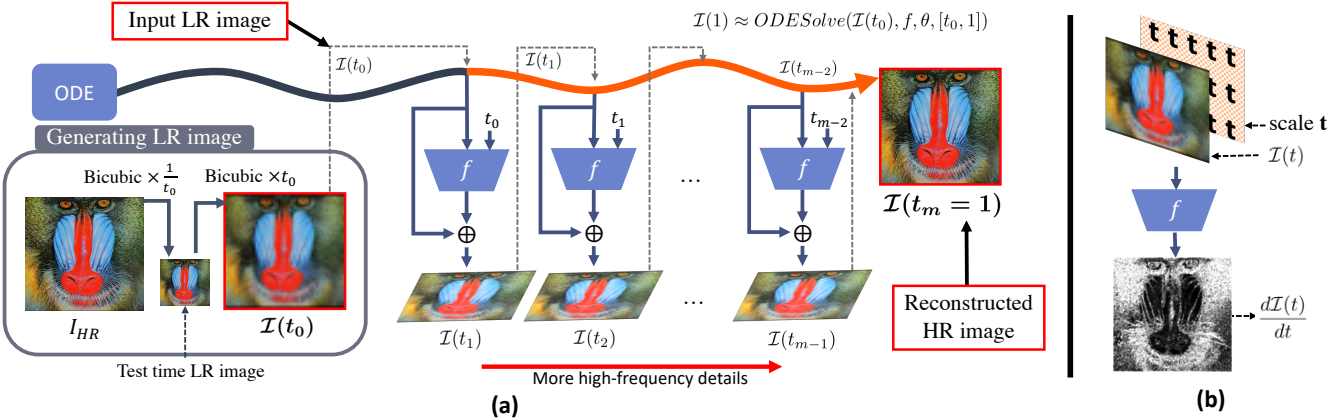


Figure 1: (a) Overview of the proposed SR approach (NODE-SR). $\{t_i\}_{0 \leq i \leq m}$ is a strictly decreasing sequence and $t_m = 1$. Solid orange line represents our SR process that starts with the initial condition $\mathcal{I}(t_0)$ until we reconstruct the final HR image $\mathcal{I}(1)$. (b) The neural network f takes an input image $\mathcal{I}(t)$ with the scale factor t and outputs the desired high-frequency detail.

Notably, $\mathcal{I}(t-1)$ includes more high-frequency details than $\mathcal{I}(t)$ without loss of generality. In our method, we model the slightest image difference to formulate a continuously progressive SR process. Therefore, we take the scale factor t to continuous domain, and reformulate (2) as an ODE with a neural network f as:

$$\frac{d\mathcal{I}(t)}{dt} = f(\mathcal{I}(t), t, \theta), \quad (3)$$

where θ denotes the trainable parameter of the network f . Using this formulation, we can predict the high-frequency image detail required to slightly enhance $\mathcal{I}(t)$ with the network f . (Note that we can obtain $\mathcal{I}(t)$ with any rational number t by adding padding to the border of image before resizing and then center cropping the image.) As existing SR neural networks have been proven to be successful at predicting the high-frequency residual image [Kim *et al.*, 2016b], we can use conventional SR architectures as our network f in (3) without major changes.

3.2 Single Image Super-Resolution with Neural Ordinary Differential Equation

In this section, we explain how to super-resolve a given LR image with a continuous scaling factor using our ODE-based SR formulation in (3).

First, we obtain $\mathcal{I}(t_0)$ by upscaling the given LR input image (“Test time LR image” in Figure 1(a)) using the bicubic SR kernel to a desired output resolution with a scaling factor t_0 . Next, we solve the ODE initial value problem in (3) with the initial condition $\mathcal{I}(t_0)$ by integrating the neural network f from t_0 to 1 to acquire the high-quality image $\mathcal{I}(1)$ as follows:

$$\mathcal{I}(1) = \mathcal{I}(t_0) + \int_{t_0}^1 f(\mathcal{I}(t), t, \theta) dt. \quad (4)$$

As the neural network f is modeled to predict desired high-frequency details, our formulation in (4) gradually adds the predicted fine details from the input LR image $\mathcal{I}(t_0)$ through the integration shown as the solid orange line in Figure 1(a).

Thus, our SR approach becomes a progressive SR process which adds the high-frequency details gradually. To compute the integration with f in the proposed formulation, we use conventional ODE solvers to numerically calculate the output image $\mathcal{I}(1)$. Specifically, we approximate the high-quality image $\mathcal{I}(1)$ given a fully trained neural network f , network parameter θ , initial condition $\mathcal{I}(t_0)$, and integral interval $[t_0, 1]$ using an ODE solver ($\text{ODESolve}()$) as:

$$\mathcal{I}(1) \approx \text{ODESolve}(\mathcal{I}(t_0), f, \theta, [t_0, 1]). \quad (5)$$

Thus, our method does not need to consider the stop condition (i.e., the number of feedback iterations) of the progressive SR process unlike conventional approaches [Tai *et al.*, 2017; Li *et al.*, 2019]. Notably, we can use conventional ODE solvers to render the desired outputs for the inference, but the solutions should be differentiable to train the network f through the backpropagation scheme. We compare the SR performance with different ODE solvers (e.g., Runge-Kutta and Euler methods) in our experiments.

Our formulation is made upon a continuous context, allows a continuous scale factor t_0 where $t_0 \geq 1$. This makes our method able to handle the arbitrary-scale SR problem. But unlike conventional multi-scale SR methods [Kim *et al.*, 2016b; Lim *et al.*, 2017; Hu *et al.*, 2019] that successfully learn multi-scale SR tasks by sharing common features across various scales, we explicitly learn the relationship between images with different scales in image domain itself rather than the feature space.

3.3 Training

To train the deep neural network f , and learn the parameter θ in (5), we minimize the loss summed over scale factors t using the L1 loss function as:

$$\mathcal{L}(\theta) = \sum_t \|I_{HR} - \text{ODESolve}(\mathcal{I}(t), f, \theta, [t, 1])\|_1. \quad (6)$$

By minimizing the proposed loss function, our network parameter θ is trained to estimate the image detail to be added into the network input as in (3).

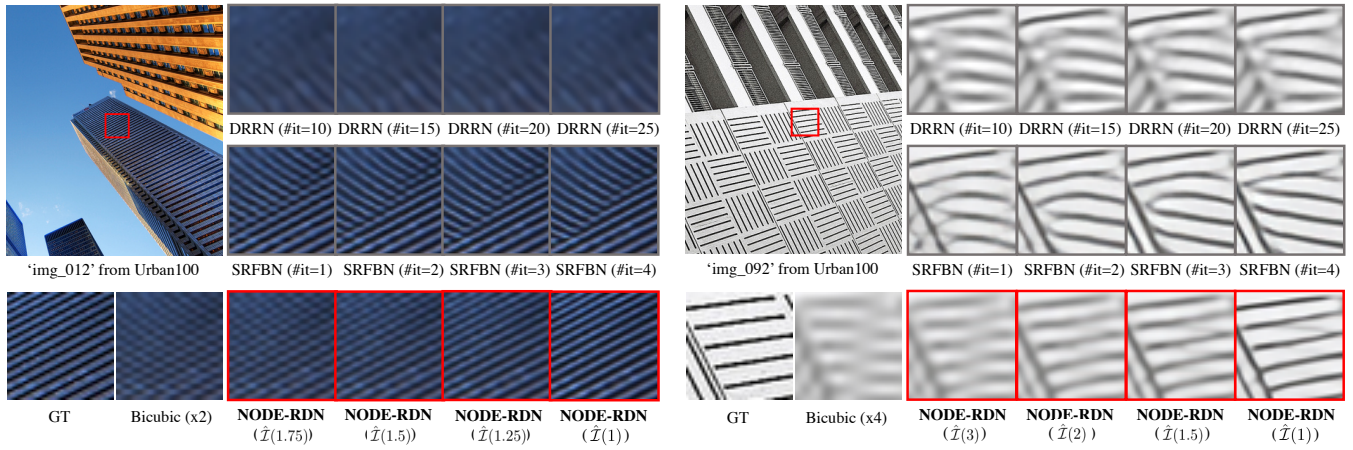


Figure 2: Visual comparisons with conventional progressive SR methods (DRRN, SRFBN). For different scale factors (x2, and x4) intermediate HR images are visualized, and #it indicates the number of updates used to render results by DRRN and SRFBN. $\hat{f}()$ denotes the predicted results by our NODE-RDN.

Dataset	Scale	Bicubic	DRCN	LapSRN	DRRN	D-DBPN	SRFBN	NODE-RDN (ours)	NODE-RDN+ (ours)
Set14	x2	30.24/0.8688	33.04/0.9118	33.08/0.913	33.23/0.9136	33.85/0.9190	33.82/0.9196	33.90/0.9209	33.95/0.9214
	x3	27.55/0.7742	29.76/0.8311	29.87/0.833	29.96/0.8349	-/-	30.51/0.8461	30.53/0.8465	30.59/0.8473
	x4	26.00/0.7027	28.02/0.7670	28.19/0.772	28.21/0.7721	28.82/0.7860	28.81/0.7868	28.76/0.7866	28.83/0.7877
B100	x2	29.56/0.8431	31.85/0.8942	31.80/0.895	32.05/0.8973	32.27/0.9000	32.29/0.9010	32.34/0.9025	32.38/0.9028
	x3	27.21/0.7385	28.80/0.7963	28.81/0.797	28.95/0.8004	-/-	29.24/0.8084	29.25/0.8094	29.28/0.8100
	x4	25.96/0.6675	27.23/0.7233	27.32/0.728	27.38/0.7284	27.72/0.7400	27.72/0.7409	27.72/0.7410	27.75/0.7417
Urban100	x2	26.88/0.8403	30.75/0.9133	30.41/0.910	31.23/0.9188	32.55/0.9775	32.62/0.9328	32.81/0.9345	32.97/0.9355
	x3	24.46/0.7349	27.15/0.8276	27.06/0.827	27.53/0.8378	-/-	28.73/0.8641	28.81/0.8644	28.94/0.8662
	x4	23.14/0.6577	25.14/0.7510	25.21/0.756	25.44/0.7638	26.38/0.7946	26.60/0.8015	26.56/0.7985	26.68/0.8010

Table 1: Comparison with progressive SR methods on the benchmark datasets (Set14, B100, and Urban100). We provide average PSNR/SSIM values for scaling factors x2, x3, and x4. Our NODE-RDN and NODE-RDN+ show the best performance. Red and blue colors denote the best and second best results, respectively.

Notably, during the training phase, we need to employ an ODE solver which allows end-to-end training using back-propagation with other components such as the neural network f . Unlike other progressive SR methods [Kim *et al.*, 2016a; Li *et al.*, 2019], we do not require any other learning strategies like curriculum learning during the training phase.

4 Experimental Results

In this section, we carry out extensive experiments to demonstrate the superiority of the proposed method, and add various quantitative and qualitative comparison results. We also provide detailed analysis of our experimental results. We will release our source code upon acceptance.

4.1 Implementation details

Network configuration. We use VDSR [Kim *et al.*, 2016b] and RDN [Zhang *et al.*, 2018] as backbone CNN architectures for our network f with slight modifications.

For each CNN architecture, we change the first layer to feed the scale factor t as an additional input. To be specific, we extend the input channel from 3 to 4, and the pixel locations of the newly concatenated channel (4-th channel) are filled with a scalar value t as shown in Figure 1(b). In addition, for RDN, we remove the last upsampling layer so that input and output resolutions are the same in our work. Note

that, no extra parameters are added except for the first layers of the networks.

To train and infer the proposed SR process, we use the Python `torchdiffeq` library [Chen *et al.*, 2018] to employ Runge–Kutta (RK4) method as our ODE solver in (6), which requires only 6 additional lines of code with PyTorch.

For simplicity, our approaches with VDSR and RDN backbones are called NODE-VDSR and NODE-RDN in the remaining parts of the experiments, respectively.

Dataset and evaluation. We use the DIV2K [Agustsson and Timofte, 2017] dataset to train our NODE-VDSR and NODE-RDN. During the training phase, we augment the dataset using random cropping, rotating, and flipping.

During the test phase, we evaluate the SR results in terms of PSNR and SSIM metrics on the standard benchmark datasets (Set14 [Zeyde *et al.*, 2010], B100 (BSD100) [Martin *et al.*, 2001], and Urban100 [Huang *et al.*, 2015]). To be consistent with previous works, quantitative results are evaluated on the Y (luminance) channel in the YCbCr color space.

Training setting. We train the network by minimizing the L1 loss in (6) with the Adam optimizer ($\beta_1 = 0.9$, $\beta_2 = 0.999$, $\epsilon = 10^{-8}$) [Kingma and Ba, 2015]. The initial learning rate is set as 10^{-4} , which is then decreased by half every 100k gradient update steps, and trained for 600k iterations in total. The mini-batch size of NODE-VDSR is 16 (200x200

Methods	Scale	x1.1	x1.2	x1.3	x1.4	x1.5	x1.6	x1.7	x1.8	x1.9	x2.0	x2.1	x2.2	x2.3	x2.4	x2.5
bicubic		36.56	35.01	33.84	32.93	32.14	31.49	30.90	30.38	29.97	29.55	29.18	28.87	28.57	28.31	28.13
VDSR		-	-	-	-	-	-	-	-	-	-	-	-	-	-	-
VDSR+t		39.51	38.44	37.15	36.04	34.98	34.15	33.39	32.78	32.22	31.70	31.27	30.86	30.53	30.2	29.91
NODE-VDSR (ours)		41.46	39.36	37.75	36.51	35.38	34.49	33.70	33.07	32.50	31.95	31.52	31.09	30.76	30.42	30.12
RDN		-	-	-	-	-	-	-	-	32.34	-	-	-	-	-	-
RDN+t		42.83	39.92	38.18	36.87	35.71	34.80	33.99	33.34	32.77	32.22	31.76	31.33	30.99	30.64	30.34
Meta-RDN		42.82	40.04	38.28	36.95	35.86	34.90	34.13	33.45	32.86	32.35	31.82	31.41	31.06	30.62	30.45
NODE-RDN (ours)		43.22	40.06	38.35	37.02	35.86	34.95	34.14	33.47	32.89	32.34	31.89	31.46	31.12	30.76	30.46
NODE-RDN+ (ours)		43.33	40.13	38.40	37.07	35.90	34.99	34.17	33.50	32.93	32.38	31.93	31.50	31.16	30.80	30.50
Methods	Scale	x2.6	x2.7	x2.8	x2.9	x3.0	x3.1	x3.2	x3.3	x3.4	x3.5	x3.6	x3.7	x3.8	x3.9	x4.0
bicubic		27.89	27.66	27.51	27.31	27.19	26.98	26.89	26.59	26.60	26.42	26.35	26.15	26.07	26.01	25.96
VDSR		-	-	-	-	28.83	-	-	-	-	-	-	-	-	-	27.29
VDSR+t		29.64	29.39	29.15	28.93	28.74	28.55	28.38	28.22	28.05	27.89	27.76	27.58	27.47	27.34	27.20
NODE-VDSR (ours)		29.85	29.61	29.36	29.14	28.94	28.75	28.58	28.41	28.25	28.08	27.96	27.79	27.66	27.54	27.40
RDN		-	-	-	-	29.26	-	-	-	-	-	-	-	-	-	27.72
RDN+t		30.06	29.80	29.55	29.33	29.12	28.92	28.76	28.59	28.43	28.26	28.13	27.95	27.84	27.71	27.58
Meta-RDN		30.13	29.82	29.67	29.40	29.30	28.87	28.79	28.68	28.54	28.32	28.27	28.04	27.92	27.82	27.75
NODE-RDN (ours)		30.18	29.93	29.67	29.45	29.25	29.05	28.88	28.71	28.54	28.37	28.24	28.07	27.96	27.81	27.72
NODE-RDN+ (ours)		30.22	29.97	29.71	29.49	29.28	29.05	28.92	28.74	28.58	28.41	28.28	28.12	28.00	27.87	27.75

Table 2: Average PSNR values on the B100 dataset evaluated with different scale factors. The best performance is shown in **bold number**.

patches), but our NODE-VDSR takes 8 patches as a mini-batch (130x130 patches) owing to the memory limit of our graphic units. Similar to the training settings in Meta-SR [Hu *et al.*, 2019], we train the network f by randomly changing the scale factor t in (6) from 1 to 4 with a stride of 0.1 (i.e., $t \in \{1.1, 1.2, 1.3, \dots, 4\}$).

4.2 Comparison with Progressive SR Methods

First, we compare our NODE-RDN with several state-of-the-art progressive SR methods: DRCN [Kim *et al.*, 2016a], LapSRN [Lai *et al.*, 2017], DRRN [Tai *et al.*, 2017], D-DPBN [Haris *et al.*, 2018], and SRFBN [Li *et al.*, 2019]. As in [Lim *et al.*, 2017], self-ensemble method is used to further improve NODE-RDN (denoted as NODE-RDN+). Note that, our NODE-RDN and NODE-RDN+ can handle multiple scale factors t including non-integer scale factors (e.g., x1.5) using the same network parameter. In contrast, other approaches are required to be trained for certain discrete integer scale factors (x2, x3, and x4) separately, resulting in a distinct parameter set for each scale factor. Nevertheless, quantitative restoration results in Table 1 show that our NODE-RDN, NODE-RDN+ consistently outperforms conventional progressive SR methods for the discrete integer scaling factors (x2, x3, and x4) in terms of PSNR.

In Figure 2, we investigate intermediate images produced during the progressive SR process with the scale factors x2 and x4. Final results by DRRN are obtained after 25 iterations, and the final results by SRFBN are obtained with 4 iterations as in their original settings. We provide 4 intermediate HR images during the updates for visual comparisons. For our NODE-RDN, intermediate image states are represented as $\hat{\mathcal{I}}(t_i)$ where $1 \leq t_i \leq t_0$ and $\hat{\mathcal{I}}(t_i) = \text{ODESolve}(\mathcal{I}(t_0), f, \theta, [t_0, t_i])$. We observe that DRRN and SRFBN fail to progressively refine patches with high-frequency details, while our NODE-RDN can gradually improve the intermediate images and render promising results at the final states.

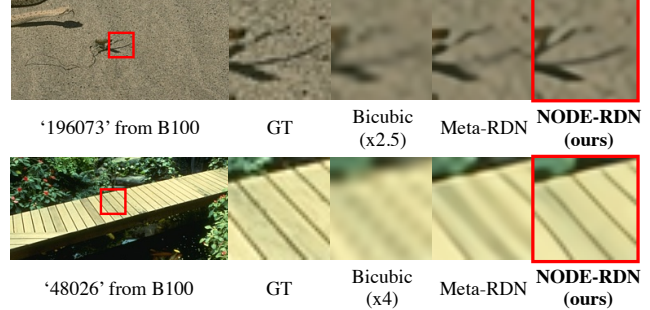


Figure 3: Visual comparison of NODE-RDN (ours) with Meta-RDN on scale x2.5 and x4.

4.3 Comparison with Multi-scale SR Methods

Our approach can handle a continuous scale factor for the SR task, thus we compare ours with existing multi-scale SR methods that can handle continuous scale factors: VDSR [Kim *et al.*, 2016b] and Meta-SR [Hu *et al.*, 2019]. Notably, Meta-SR implemented using RDN (i.e., Meta-RDN) is the current state-of-the-art SR approach.

In Table 2, we show quantitative results compared to existing SR methods (VDSR, RDN, and Meta-RDN). Note that, VDSR+t and RDN+t are modified versions of VDSR and RDN to take the scale factor t as an additional input of the networks and have the same input and output resolutions as in our network f . We also compare our method with these new baselines (VDSR+t and RDN+t) for fair comparisons.

We evaluate the SR performance on the B100 benchmark dataset by increasing the scaling factor from 1.1 to 4.

Interestingly, we observe that NODE-VDSR outperforms VDSR and VDSR+t at every scale by a large margin although VDSR and VDSR+t have similar network architecture to our NODE-VDSR. Similarly, NODE-RDN shows better performance than Meta-RDN and RDN+t. We also provide qualitative comparison results with Meta-SR in Figure 3, and we

	Euler Method			Runge-Kutta Method		
	x2	x3	x4	x2	x3	x4
B100	31.92	28.89	27.33	31.96	28.94	27.38
Set5	37.57	33.92	31.50	37.58	34.03	31.68

Table 3: Benchmark results of NODE-VDSR trained with Euler and Runge-Kutta methods on different scale factors. **Bold number** indicates better SR performance.

see that our NODE-RDN recovers much clearer edges than Meta-RDN.

4.4 Detailed Analysis

Interpolation and extrapolation. We experiment our method on various scale factors that are not shown during the training phase. In Figure 4, we plot PSNR values from NODE-VDSR and NODE-RDN by changing the scale factor on the B100 dataset. We see that our method learns an interpolation ability and can successfully deal with unseen scales between 1 and 4 (e.g., 1.15, 1.25, ..., 3.95). Moreover, ours also learns an extrapolation ability and handles unseen scale factors larger than 4 (e.g., 4.1, 4.2, ..., 4.5). To sum up, our proposed SR process has a power of generalization (i.e., interpolation and extrapolation abilities), even the network is trained with only a limited number of scale factors.

SR performance with different ODE solvers. We experiment our method with different ODE solvers (e.g., Euler and RK4 methods). Note that Euler method is computationally cheaper than RK4, but RK4 provides more accurate approximation results generally. Similarly, in Table 3, we see that NODE-VDSR trained with RK4 shows slightly better SR performance than NODE-VDSR trained with Euler method on the B100 and Set5 datasets. This result suggests that, we can employ conventional ODE solvers to solve our own SR problem, but the quality of the predicted HR images are relying on the performance of the employed ODE solver.

Visual output of the network f . In Figure 5, to see the intermediate results by the network f during the progressive SR procedure at the test stage, we compute absolute value of $f(\hat{\mathcal{I}}(t), t, \theta)$ where t decreases from 4 to 1, and the initial condition is $\mathcal{I}(t_0 = 4)$.

Interestingly, on the sharp patch corresponding to the eye (red box), the absolute values are higher when t is small. While, on the homogeneous patch corresponding to the cheek (green box), the absolute values are higher when t is large. Recall that $\mathcal{I}(t)$ becomes close to the ground-truth image when t gets small, and the image difference $\frac{d\mathcal{I}(t)}{dt}$ ($\approx f(\hat{\mathcal{I}}(t), t, \theta)$) includes more high-frequency components. Therefore, the absolute values of the network at the eye region which includes high-frequency detail becomes large when t is small, while the absolute values at the homogeneous region which does not require high-frequency detail becomes small when t is small.

5 Conclusion

In this work, we proposed a novel differential equation for the SR task to progressively enhance a given input LR image, and

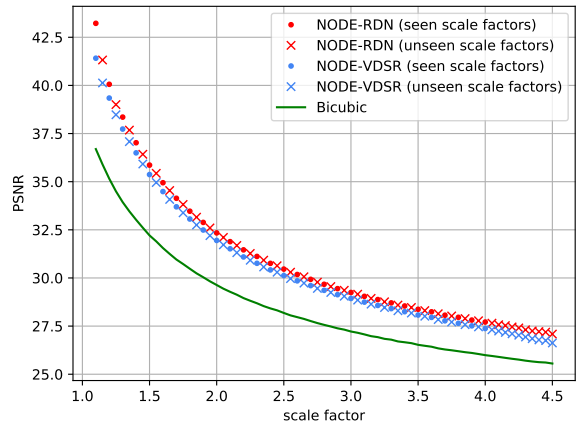


Figure 4: PSNR evaluations of bicubic upscaling, NODE-VDSR, and NODE-RDN on the B100 dataset by changing the scale factor from 1.1 to 4.5 with stride 0.05. Dotted marks correspond to seen scale factors during the training process (e.g., 1.1, 1.2, ..., 4.0) and cross marks correspond to unseen scale factors (e.g., 1.15, 1.25, ..., 4.5) during the training.

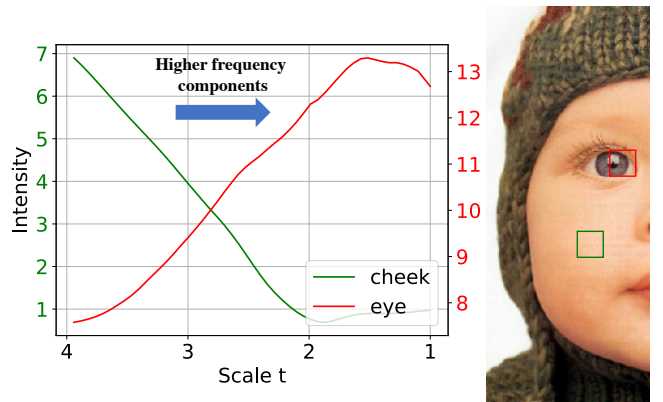


Figure 5: Intensity of intermediate image derivatives by changing scale factor t at two different locations.

allow continuous-valued scale factor. Image difference between images over different scale factors is physically modeled with a neural network, and formulated as a NODE. To restore a high-quality image, we solve the ODE initial value problem with the initial condition given as an input LR image. The main difference with existing progressive SR methods is that our formulation is based on the physical modeling of the intermediate images, and adds fine high-frequency details gradually. The analysis on the intermediate states during the SR process gives us more insight on the progressive SR reconstruction. Detailed experimental results show that our method achieves superior performance compared to state-of-the-art SR approaches.

References

[Agustsson and Timofte, 2017] Eirikur Agustsson and Radu Timofte. Ntire 2017 challenge on single image super-resolution: Dataset and study. 2017.

[Cai *et al.*, 2019] Jianrui Cai, Hui Zeng, Hongwei Yong, Zisheng Cao, and Lei Zhang. Toward real-world single image super-resolution: A new benchmark and a new model. In *Proceedings of the IEEE International Conference on Computer Vision*, 2019.

[Chen and Pock, 2016] Yunjin Chen and Thomas Pock. Trainable nonlinear reaction diffusion: A flexible framework for fast and effective image restoration. *IEEE transactions on pattern analysis and machine intelligence*, 2016.

[Chen *et al.*, 2005] Yuanxu Chen, Yupin Luo, and Dongcheng Hu. A general approach to blind image super-resolution using a pde framework. In *Visual Communications and Image Processing 2005*. International Society for Optics and Photonics, 2005.

[Chen *et al.*, 2018] Ricky TQ Chen, Yulia Rubanova, Jesse Bettencourt, and David K Duvenaud. Neural ordinary differential equations. In *Advances in neural information processing systems*, 2018.

[Dong *et al.*, 2015] Chao Dong, Chen Change Loy, Kaiming He, and Xiaoou Tang. Image super-resolution using deep convolutional networks. *IEEE transactions on pattern analysis and machine intelligence*, 38(2), 2015.

[Haris *et al.*, 2018] Muhammad Haris, Gregory Shakhnarovich, and Norimichi Ukita. Deep back-projection networks for super-resolution. In *Proceedings of the IEEE conference on computer vision and pattern recognition*, 2018.

[He *et al.*, 2019] Xiangyu He, Zitao Mo, Peisong Wang, Yang Liu, Mingyuan Yang, and Jian Cheng. Ode-inspired network design for single image super-resolution. In *Proceedings of the IEEE Conference on Computer Vision and Pattern Recognition*, 2019.

[Hu *et al.*, 2019] Xuecai Hu, Haoyuan Mu, Xiangyu Zhang, Zilei Wang, Tieniu Tan, and Jian Sun. Meta-sr: A magnification-arbitrary network for super-resolution. In *Proceedings of the IEEE Conference on Computer Vision and Pattern Recognition*, 2019.

[Huang *et al.*, 2015] Jia-Bin Huang, Abhishek Singh, and Narendra Ahuja. Single image super-resolution from transformed self-exemplars. In *Proceedings of the IEEE conference on computer vision and pattern recognition*, 2015.

[Kim *et al.*, 2016a] Jiwon Kim, Jung Kwon Lee, and Kyoung Mu Lee. Deeply-recursive convolutional network for image super-resolution. In *Proceedings of the IEEE conference on computer vision and pattern recognition*, 2016.

[Kim *et al.*, 2016b] Jiwon Kim, Jung Kwon Lee, and Kyoung Mu Lee. Accurate image super-resolution using very deep convolutional networks. In *Proceedings of the IEEE conference on computer vision and pattern recognition*, 2016.

[Kingma and Ba, 2015] Diederik P. Kingma and Jimmy Ba. Adam: A method for stochastic optimization. In *International Conference on Learning Representations*, 2015.

[Lai *et al.*, 2017] Wei-Sheng Lai, Jia-Bin Huang, Narendra Ahuja, and Ming-Hsuan Yang. Deep laplacian pyramid networks for fast and accurate super-resolution. In *Proceedings of the IEEE conference on computer vision and pattern recognition*, 2017.

[Li *et al.*, 2019] Zhen Li, Jinglei Yang, Zheng Liu, Xiaomin Yang, Gwanggil Jeon, and Wei Wu. Feedback network for image super-resolution. In *Proceedings of the IEEE Conference on Computer Vision and Pattern Recognition*, 2019.

[Lim *et al.*, 2017] Bee Lim, Sanghyun Son, Heewon Kim, Seungjun Nah, and Kyoung Mu Lee. Enhanced deep residual networks for single image super-resolution. In *Proceedings of the IEEE conference on computer vision and pattern recognition workshops*, 2017.

[Martin *et al.*, 2001] David Martin, Charless Fowlkes, Doron Tal, and Jitendra Malik. A database of human segmented natural images and its application to evaluating segmentation algorithms and measuring ecological statistics. In *Proceedings of the IEEE International Conference on Computer Vision*. IEEE, 2001.

[Rudin *et al.*, 1992] Leonid I Rudin, Stanley Osher, and Emad Fatemi. Nonlinear total variation based noise removal algorithms. *Physica D: nonlinear phenomena*, 1992.

[Scao, 2020] Teven Le Scao. Neural differential equations for single image super-resolution. In *ICLR 2020 Workshop on Integration of Deep Neural Models and Differential Equations*, 2020.

[Tai *et al.*, 2017] Ying Tai, Jian Yang, and Xiaoming Liu. Image super-resolution via deep recursive residual network. In *Proceedings of the IEEE conference on computer vision and pattern recognition*, 2017.

[Zamir *et al.*, 2017] Amir R Zamir, Te-Lin Wu, Lin Sun, William B Shen, Bertram E Shi, Jitendra Malik, and Silvio Savarese. Feedback networks. In *Proceedings of the IEEE Conference on Computer Vision and Pattern Recognition*. IEEE, 2017.

[Zeyde *et al.*, 2010] Roman Zeyde, Michael Elad, and Matan Protter. On single image scale-up using sparse-representations. In *International conference on curves and surfaces*. Springer, 2010.

[Zhang *et al.*, 2018] Yulun Zhang, Yapeng Tian, Yu Kong, Bineng Zhong, and Yun Fu. Residual dense network for image super-resolution. In *Proceedings of the IEEE conference on computer vision and pattern recognition*, 2018.